

Growth, Annealing Effects on Superconducting and Magnetic Properties and Anisotropy of $\text{FeSe}_{1-x}\text{Te}_x$ ($0.5 \leq x \leq 1$) Single Crystals

Takashi Noji, Takumi Suzuki, Haruki Abe, Tadashi Adachi, Masatsune Kato, and Yoji Koike
Department of Applied Physics, Tohoku University, Sendai 980-8579

Single crystals of $\text{FeSe}_{1-x}\text{Te}_x$ ($0.5 \leq x \leq 1$) have been grown by the Bridgman method. After annealing them at 400°C for 100 h in vacuum, single crystals of $x = 0.5 - 0.9$ have exhibited bulk superconductivity. Anisotropic properties of the electrical resistivity and upper critical field, H_{c2} , have been investigated for the single-crystal $\text{FeSe}_{1-x}\text{Te}_x$ with $x = 0.6$. It has been found that the in-plane resistivity, ρ_{ab} , shows a metallic temperature-dependence, while the out-of-plane resistivity, ρ_c , shows a broad maximum around 100 K. The resistivity ratio, ρ_{ab}/ρ_c , is 44 and 70 at 290 K and just above the superconducting transition temperature, T_c , respectively. The anisotropic parameter, $\gamma \equiv H_{c2}^{\parallel}/H_{c2}^{\perp}$ (The superscripts \parallel and \perp indicate field directions parallel and perpendicular to the ab-plane, respectively.), is estimated as 2.7 just below T_c .

KEYWORDS

$\text{FeSe}_{1-x}\text{Te}_x$ single crystal, annealing effect, anisotropy, electrical resistivity, upper critical field

I . Introduction

The discovery of superconductivity at 26 K in the iron-based oxypnictide superconductor $\text{LaFeAsO}_{1-x}\text{F}_x$ is quite surprising,¹⁾ since compounds including iron are usually so magnetic as not to be superconducting. To the surprise, moreover, the superconducting transition temperature, T_c , has been raised up to 55 K by replacing La with other rare-earth elements such as Sm.²⁾ After that Hsu *et al.* have discovered superconductivity with $T_c = 8$ K in the PbO-type structure FeSe.³⁾ This has also attracted great interest, because the crystal structure is so simple as to be composed of a stack of edge-sharing FeSe_4 -tetrahedra layers which are similar to FeAs_4 -tetrahedra layers in $\text{LaFeAsO}_{1-x}\text{F}_x$, and because T_c of FeSe has markedly increased up to 37 K by the application of high pressure of 7 GPa.⁴⁾ It has been found that T_c of FeSe increases through the partial substitution of Te for Se as well, shows a maximum 14 K at $x = 0.6$ in $\text{FeSe}_{1-x}\text{Te}_x$ and the superconductivity disappears at $x = 1$, namely, in FeTe.^{5,6)} The end member FeTe is not superconducting but develops an antiferromagnetic order at low temperatures below ~ 67 K where a tetragonal-to-monoclinic structural phase transition occurs.^{7,8)} As for the single-crystal growth of $\text{FeSe}_{1-x}\text{Te}_x$, tiny crystals of FeSe with a size of ~ 500 μm and $T_c = 10.4$ K have been obtained using a NaCl/KCl flux.⁹⁾ Recently, large-sized single-crystals of Fe_{1+y}Te and $\text{Fe}_{1+y}\text{Se}_{1-x}\text{Te}_x$ with the tetragonal structure have successfully been grown by the Bridgman method.¹⁰⁻¹²⁾

In this paper, we report on the growth and characterization of $\text{Fe}_{1+y}\text{Se}_{1-x}\text{Te}_x$ ($0.5 \leq x \leq 1$) single crystals with y values as small as possible due to excess Fe randomly occupying the so-called Fe(2) site in the crystal structure between neighboring square planar sheets of Fe.⁷⁾ Annealing effects on the superconducting and magnetic properties of $\text{Fe}_{1+y}\text{Se}_{1-x}\text{Te}_x$ ($0.5 \leq x \leq 1$) single crystals are also investigated. Moreover, anisotropic properties of the electrical resistivity and upper critical field, H_{c2} , of the annealed single-crystal $\text{FeSe}_{1-x}\text{Te}_x$ with $x = 0.6$ are investigated.

II . Experimental

Single crystals of $\text{FeSe}_{1-x}\text{Te}_x$ were grown by the Bridgman method. Starting materials were powders of Fe (purity 3N), Se (purity 3N) and Te (purity 4N). The powders prescribed in the nominal composition described in Table I were thoroughly mixed in an argon-filled glove box. The mixed powders were sealed in an evacuated quartz tube. Since the quartz tube often cracked upon cooling, the tube was sealed into another large-sized evacuated quartz tube. The doubly sealed quartz ampoule was stood in a furnace so that single crystals were grown using the

temperature gradient in the furnace. The ampoule was heated at 600°C for 100 h and successively at 950 - 1050°C for 30 h, and then cooled down to 650°C at the rate of 2 - 3°C/h, followed by furnace cooling down to room temperature.

Grown crystals were characterized by the x-ray back-Laue photography and the powder x-ray diffraction. The chemical composition was determined by the inductively coupled plasma atomic emission spectroscopy (ICP-AES). The composition of the surface of the crystals was checked using an electron probe microanalyzer (EPMA).

The magnetic susceptibility, χ , was measured using a superconducting quantum interference device (SQUID) magnetometer (Quantum Design, Model MPMS). Measurements of the electrical resistivity were carried out by the standard DC four-probe method. The anisotropy in the resistive superconducting transition under magnetic field was measured using a commercial apparatus (Quantum Design, Model PPMS) to investigate the anisotropy of H_{c2} . Here, the magnetic field was always applied perpendicular to the direction of the excitation current flowing in the ab-plane.

III. Results and Discussion

We have succeeded in growing sizable single-crystals of $0.6 \leq x \leq 1$, but it was hard to obtain single crystals with $x = 0.5$ whose dimensions of the ab-plane are larger than $1 \text{ mm} \times 1 \text{ mm}$. As-grown crystals of $0.6 \leq x \leq 1$ were easily cloven. Figures 1 (a) and (b) show a picture of as-grown single-crystals with cleavage surface and a x-ray back-Laue photograph in the x-ray perpendicular to the cleavage surface, respectively. The fourfold symmetry in the back-Laue photograph is due to the tetragonal structure, indicating that the c-axis is perpendicular to the cleavage surface. The powder x-ray diffraction has revealed that the obtained crystals are of the single phase without any impurity phases. Compositions of the obtained crystals chemically analyzed by ICP-AES are listed in Table I. It is found that the chemical compositions of the single crystals are in approximate agreement with the nominal ones. Experimentally, it was hard to grow stoichiometric crystals of $\text{FeSe}_{1-x}\text{Te}_x$ without excess Fe.

Figure 2 shows the temperature dependence of the in-plane resistivity, ρ_{ab} , of as-grown single-crystals of $\text{FeSe}_{1-x}\text{Te}_x$ ($0.5 \leq x \leq 1$). It is found that superconductivity appears in these samples except for $x = 1$. Values of T_c are comparable with those of sintered polycrystalline

samples.^{5,6)} As for $x = 1$, namely FeTe, ρ_{ab} shows a semiconductor-like behavior at high temperatures, whereas ρ_{ab} drops steeply at ~ 65 K and then exhibits a metallic behavior at low temperatures. The discontinuous change in ρ_{ab} is due to the structural phase transition accompanied by the magnetic transition.^{7,8)}

Figure 3 shows the temperature dependence of χ in a low magnetic field of 1 mT parallel to the c-axis for as-grown and annealed single-crystals of $x = 0.5 - 0.9$. It is found that as-grown crystals of $x = 0.5$ and 0.6 display diamagnetism due to bulk superconductivity, while as-grown crystals of $x = 0.7 - 0.9$ do not. That is, the resistive superconducting transition observed in as-grown crystals of $x = 0.7 - 0.9$ is not due to bulk superconductivity. The temperature dependence of χ for as-grown single-crystals of $x = 0.8 - 1$ in a high magnetic field of 1 T parallel to the c-axis is shown in Fig. 4. It is found that the magnetic transition temperature, T_m , defined at the temperature where χ rapidly changes, decreases with decreasing x . These results suggest that a phase separation into filamentary superconducting regions and non-superconducting regions takes place in as-grown single-crystals of $x = 0.7 - 0.9$, which is consistent with the preceding result by Sales *et al.*¹¹⁾

We have annealed the as-grown crystals at 400°C for 100 h in vacuum. As seen in Fig. 3, annealed crystals of $x = 0.5 - 0.9$ exhibit bulk superconductivity, whereas as-grown crystals of $x = 0.7 - 0.9$ do not. Even for $x = 0.5$ and 0.6 , the diamagnetic signal is enhanced through the annealing. Values of T_c , defined as onset temperature of the Meissner effect, are estimated as 14.0 K, 14.2 K, 14.3 K, 13.8 K and 11.3 K for annealed crystals of $x = 0.5, 0.6, 0.7, 0.8$ and 0.9 , respectively. As seen in Fig.4, T_m of $x = 1$ increases a little up to 69 K through the annealing, while the magnetic transition of $x = 0.9$ disappears. Dependences on x of T_c and T_m for as-grown and annealed crystals are shown in Fig. 5. It seems that the distribution of Se and Te in a crystal becomes homogeneous through the annealing as pointed by Taen *et al.*,¹²⁾ so that the antiferromagnetic order observed for as-grown crystals of $x = 0.8$ and 0.9 disappears and alternatively bulk superconductivity appears for annealed single-crystals of $x = 0.7 - 0.9$. However, no structural change through the annealing could be detected by the powder x-ray diffraction. In addition, no change of the composition of the surface of the crystals through the annealing was detected by the EPMA measurements.

Figure 6 shows the temperature dependence of ρ_{ab} and the out-of-plane resistivity, ρ_c , and the resistivity ratio, ρ_c/ρ_{ab} , for the single crystal of $x = 0.6$ annealed at 400°C for 100 h in vacuum.

The ρ_{ab} shows a metallic temperature-dependence at low temperatures below 140 K, while it is nearly constant at high temperatures above 140 K. This behavior of ρ_{ab} is almost the same as that observed by Taen *et al.*¹²⁾ in the single-crystal $\text{FeTe}_{0.61}\text{Se}_{0.39}$. On the other hand, ρ_c is semiconductor-like at high temperatures, shows a broad maximum around 100 K and changes to be metallic at low temperatures below ~ 100 K. The resistivity ratio increases with decreasing temperature, while it is nearly constant at low temperatures below ~ 50 K. The resistivity ratio is 44 and 70 at 290 K and just above T_c , respectively. These values are much smaller than those of the high- T_c cuprate $\text{Bi}_2\text{Sr}_2\text{CaCu}_2\text{O}_8$ whose single-crystals are cloven as easily as $\text{FeSe}_{1-x}\text{Te}_x$ single crystals.¹³⁾ The anisotropic behaviors of ρ_{ab} and ρ_c are similar to those observed in the layered perovskite Sr_2RuO_4 .^{14,15)} As in the case of Sr_2RuO_4 , this compound is regarded as a two-dimensional metal at high temperatures above ~ 100 K, while it becomes an anisotropic three-dimensional metal at low temperatures below ~ 100 K.

Figure 7 shows the angular dependence of ρ_{ab} in various constant fields at a temperature just below T_c for the single crystal of $x = 0.6$ annealed at 400°C for 100 h in vacuum. The H_{c2} is defined at the intersection between ρ_{ab} and the half of the normal-state value of ρ_{ab} in zero field. The angular dependence of H_{c2} obtained thus is shown in Fig. 8. This is well expressed as $H_{c2}(\theta) = H_{c2}^{\parallel} (\cos^2\theta + \gamma^2 \sin^2\theta)^{-1/2}$, based on the effective mass model.¹⁶⁾ Here, θ is the angle between the ab-plane and the field direction and γ is the anisotropy parameter defined as $\gamma \equiv H_{c2}^{\parallel}/H_{c2}^{\perp}$. Here, the superscripts \parallel and \perp indicate the field direction parallel and perpendicular to the ab-plane, respectively. The fitting parameter γ obtained is 2.7.

This value of γ is larger than those of $\text{FeSe}_{1-x}\text{Te}_x$ reported so far. That is, γ is estimated as 1.6 for $\text{FeSe}_{1-x}\text{Te}_x$ with $x = 0.7$ by Chen *et al.*¹⁰⁾ and as less than 2 near T_c and decreasing with a decrease of temperature for $\text{Fe}_{1.11}\text{Se}_{1-x}\text{Te}_x$ with $x = 0.6$ by Fang *et al.*¹⁷⁾ Our large value of γ may be due to the good quality of our crystal owing to the annealing. In any case, our value of γ is similar to those of $\text{Ba}_{1-x}\text{K}_x\text{Fe}_2\text{As}_2$ ^{18,19)} and much smaller than the smallest value of $\gamma = 5$ in $\text{YBa}_2\text{Cu}_3\text{O}_y$ among the high- T_c cuprates.²⁰⁾ This suggests that the Fermi-surface topology of $\text{FeSe}_{1-x}\text{Te}_x$ is similar to that of $\text{Ba}_{1-x}\text{K}_x\text{Fe}_2\text{As}_2$ and more or less three-dimensional and different from that of

high- T_c cuprates.

Finally, it is noted that the value of γ is able to be estimated from the value of ρ_c/ρ_{ab} as $\gamma \equiv H_{c2}^{\parallel}/H_{c2}^{\perp} = (m_c^*/m_{ab}^*)^{1/2} = (\rho_c/\rho_{ab})^{1/2}$, assuming that ρ_{ab} and ρ_c are given by $m_{ab}^*/ne^2\tau$ and $m_c^*/ne^2\tau$, respectively. Here, n is the carrier concentration, e the electric charge, τ the relaxation time of carriers, and m_{ab}^* and m_c^* are the effective masses in the ab -plane and along the c -axis, respectively. The value of γ thus obtained is 8.4 just above T_c , which is larger than $\gamma = 2.7$ estimated from the anisotropy of H_{c2} . This may be due to the large value of ρ_c probably caused by the strong scattering of carriers by excess Fe. That is, τ in ρ_c may be smaller than in ρ_{ab} .

IV. Summary

Single crystals of $\text{FeSe}_{1-x}\text{Te}_x$ ($0.5 \leq x \leq 1$) were grown by the Bridgman method. The magnetic susceptibility measurements have revealed that single crystals of $x = 0.5 - 0.9$ annealed at 400°C for 100 h in vacuum exhibit bulk superconductivity, though as-grown crystals of only $x = 0.5$ and 0.6 do. It seems to be due to the homogeneous distribution of Se and Te in a crystal through the annealing. The anisotropy of the electrical resistivity and H_{c2} has been investigated for the annealed single-crystal of $\text{FeSe}_{1-x}\text{Te}_x$ with $x = 0.6$. The anisotropy in the electrical resistivity, ρ_c/ρ_{ab} , has been found to be 44 and 70 at 290 K and just above T_c , respectively. The anisotropy in H_{c2} has been estimated from the angular dependence of $\rho_{ab}(H, \theta)$ under various constant magnetic fields just below T_c . The angular dependence of H_{c2} thus obtained has been found to be explained in terms of the effective mass model, and the anisotropy parameter, $\gamma \equiv H_{c2}^{\parallel}/H_{c2}^{\perp}$, has been estimated as 2.7 just below T_c .

Acknowledgments

We would like to thank K. Takada and M. Ishikuro in Institute for Materials Research (IMR), Tohoku University, for their aid in the ICP-AES analysis. We also thank Y. Murakami in the Advanced Research Center of Metallic Glasses, IMR, Tohoku University, for his aid in the EPMA measurements. This work was supported by a Grant-in-Aid for Scientific Research from the Japan Society for the Promotion of Science.

References

- 1) Y. Kamihara, T. Watanabe, M. Hirano, and H. Hosono: *J. Am. Chem. Soc.* **130** (2008) 3296.
- 2) Z.-A. Ren, W. Lu, J. Yang, W. Yi, X.-L. Shen, Z.-C. Li, G.-C. Che, X.-L. Dong, L.-L. Sun, F. Zhou, and Z.-X. Zhao: *Chin. Phys. Lett.* **25** (2008) 2215.
- 3) F.-C. Hsu, J.-Y. Luo, K.-W. Yeh, T.-K. Chen, T.-W. Huang, P. M. Wu, Y.-C. Lee, Y.-L. Huang, Y.-Y. Chu, D.-C. Yan, and M.-K. Wu: *Proc. Nati. Acad. Sci.* **105** (2008) 14262.
- 4) S. Margadonna, Y. Takabayashi, Y. Ohishi, Y. Mizuguchi, Y. Takano, T. Kagayama, T. Nakagawa, M. Takata, and K. Prassides: *Phys. Rev. B* **80** (2009) 064506.
- 5) K.-W. Yeh, T.-W. Huang, Y.-L. Huang, T.-K. Chen, F.-C. Hsu, P. M. Wu, Y.-C. Lee, Y.-Y. Chu, C.-L. Chen, J.-Y. Luo, D.-C. Yan, and M.-K. Wu: *Europhys. Lett.* **84** (2008) 37002.
- 6) M. H. Fang, H. M. Pham, B. Qian, T. J. Liu, E. K. Vehstedt, Y. Liu, L. Spinu, and Z. Q. Mao: *Phys. Rev. B* **78** (2008) 224503.
- 7) S. Li, C. de la Cruz, Q. Huang, Y. Chen, J. W. Lynn, J. Hu, Y.-L. Huang, F.-C. Hsu, K.-W. Yeh, M.-K. Wu, and P. Dai: *Phys. Rev. B* **79** (2009) 054503.
- 8) W. Bao, Y. Qiu, Q. Huang, M. A. Green, P. Zajdel, M. R. Fitzsimmons, M. Zhernenkov, S. Chang, M. Fang, B. Qian, E. K. Vehstedt, J. Yang, H. M. Pham, L. Spinu, and Z. Q. Mao: *Phys. Rev. Lett.* **102** (2008) 247001.
- 9) S. B. Zhang, Y. P. Sun, X. D. Zhu, X. B. Zhu, B. S. Wang, G. Li, H. C. Lei, X. Luo, Z. R. Yang, W. H. Song, and J. M. Dai: *Supercond. Sci. Technol.* **22** (2009) 015020.
- 10) G. F. Chen, Z. G. Chen, J. Dong, W. Z. Hu, G. Li, X. D. Zhang, P. Zheng, J. L. Luo, and N. L. Wang: *Phys. Rev. B* **79** (2009) 140509(R).
- 11) B. C. Sales, A. S. Sefat, M. A. McGuire, R. Y. Jin, D. Mandrus, and Y. Mozharivskyj: *Phys. Rev. B* **79** (2009) 094521.
- 12) T. Taen, Y. Tsuchiya, Y. Nakajima, and T. Tamegai: *Phys. Rev. B* **80** (2009) 092502.
- 13) K. Kadowaki, A. A. Menovsky, and J. J. M. Franse: *Physica B* **165&166** (1990) 1159.
- 14) F. Lichtenberg, A. Catana, J. Mannhart, and D. G. Schlom: *Appl. Phys. Lett.* **60** (1992) 1138.
- 15) Y. Maeno, H. Hashimoto, K. Yoshida, S. Nishizaki, T. Fujita, J. G. Bednorz and F. Lichtenberg: *Nature* **372** (1994) 532.
- 16) R. C. Morris, R. V. Coleman, and R. Bhandari,: *Phys. Rev. B* **5** (1972) 895.
- 17) M. Fang, J. Yang, F. F. Balakirev, Y. Kohama, J. Singleton, B. Qian, Z. Q. Mao, H. Wang, and H. Q. Yuan: *Phys. Rev. B* **81** (2010) 020509(R).
- 18) N. Ni, S. L. Bud'ko, A. Kreyssig, S. Nandi, G. E. Rustan, A. I. Goldman, S. Gupta, J. D. Corbett,

A. Kracher, and P. C. Canfield: Phys. Rev. B **78** (2008) 014507.

19) H. Q. Yuan, J. Singleton, F. F. Balakirev, S. A. Baily, G. F. Chen, J. L. Luo, and N. L. Wang: Nature **457** (2009) 565.

20) Y. Iye, T. Tamegai, T. Sakakibara, T. Goto, N. Miura, H. Takeya, and H. Takei: Physica C **153-155** (1988) 26.

Table I . Compositions of $\text{FeSe}_{1-x}\text{Te}_x$ single crystals, and the superconducting transition temperature, T_c , and the magnetic transition temperature, T_m , for annealed single-crystals of $\text{FeSe}_{1-x}\text{Te}_x$. T_c is defined as the onset temperature of the Meissner effect.

x	nominal composition	composition (ICP-AES)	T_c^{annealed} (K)	T_m^{annealed} (K)
	Fe : Se : Te	Fe : Se : Te		
0.5	1.03 : 0.50 : 0.50	1.03 : 0.46 : 0.54	14.0	—
0.6	1.03 : 0.40 : 0.60	1.00 : 0.39 : 0.61	14.2	—
0.7	1.03 : 0.30 : 0.70	1.03 : 0.28 : 0.72	14.3	—
0.8	1.03 : 0.20 : 0.80	1.03 : 0.19 : 0.81	13.8	—
0.9	1.03 : 0.10 : 0.90	1.02 : 0.08 : 0.92	11.3	—
1	1.13 : 0 : 1.00	1.09 : 0 : 1.00	—	69

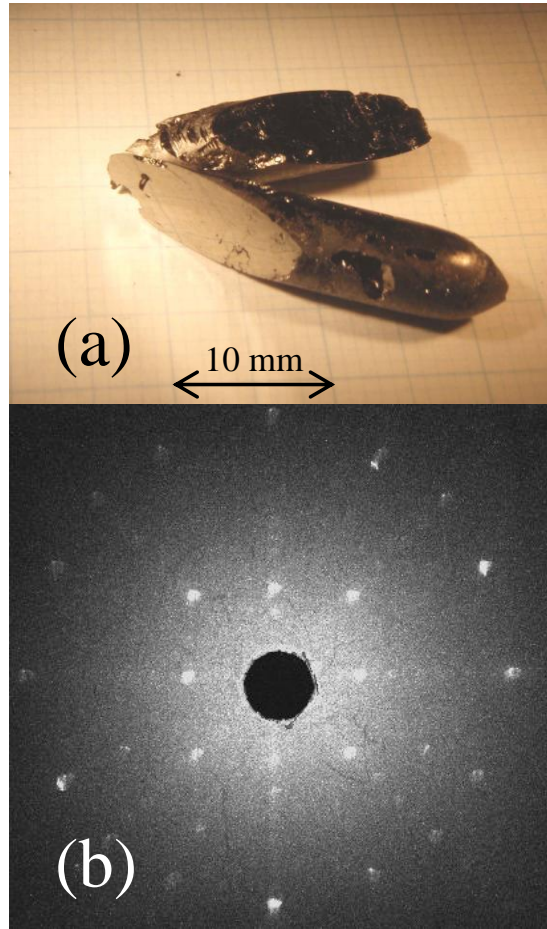


Fig. 1. (Color online) (a) Picture of as-grown single-crystals. (b) X-ray back-Laue photograph of an as-grown single-crystal of FeSe_{1-x}Te_x with $x = 0.8$ in the x-ray perpendicular to the cleavage surface, namely, the ab-plane.

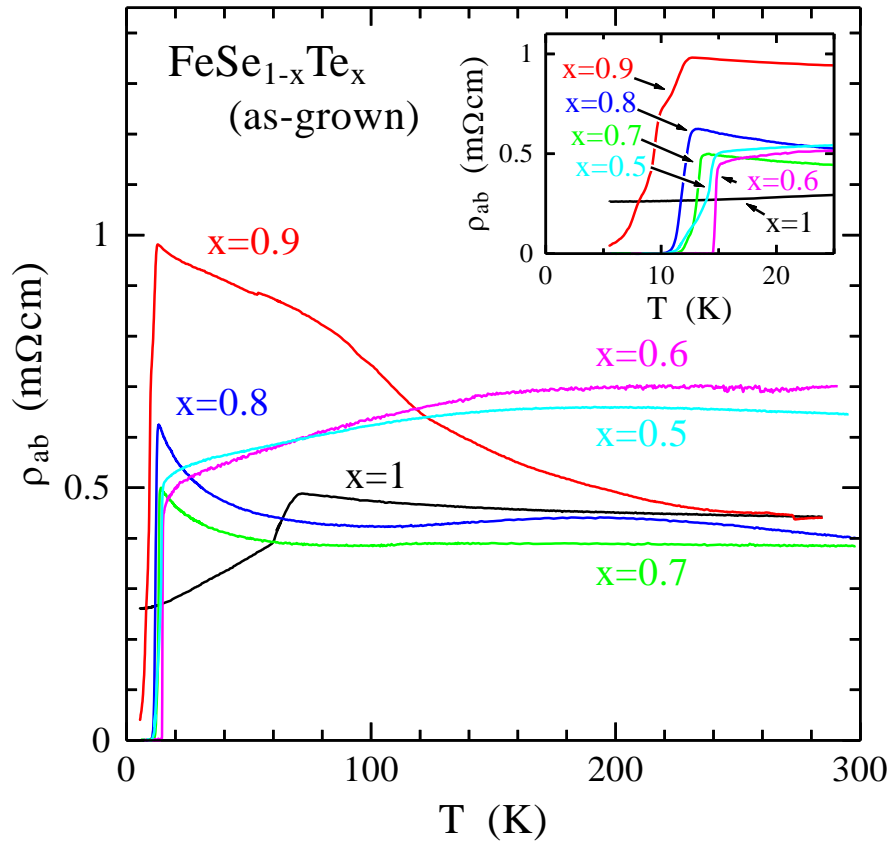


Fig. 2. (Color online) Temperature dependence of the in-plane resistivity, ρ_{ab} , of as-grown single-crystals of $\text{FeSe}_{1-x}\text{Te}_x$ ($0.5 \leq x \leq 1$). The inset is an enlarged plot of ρ_{ab} at low temperatures.

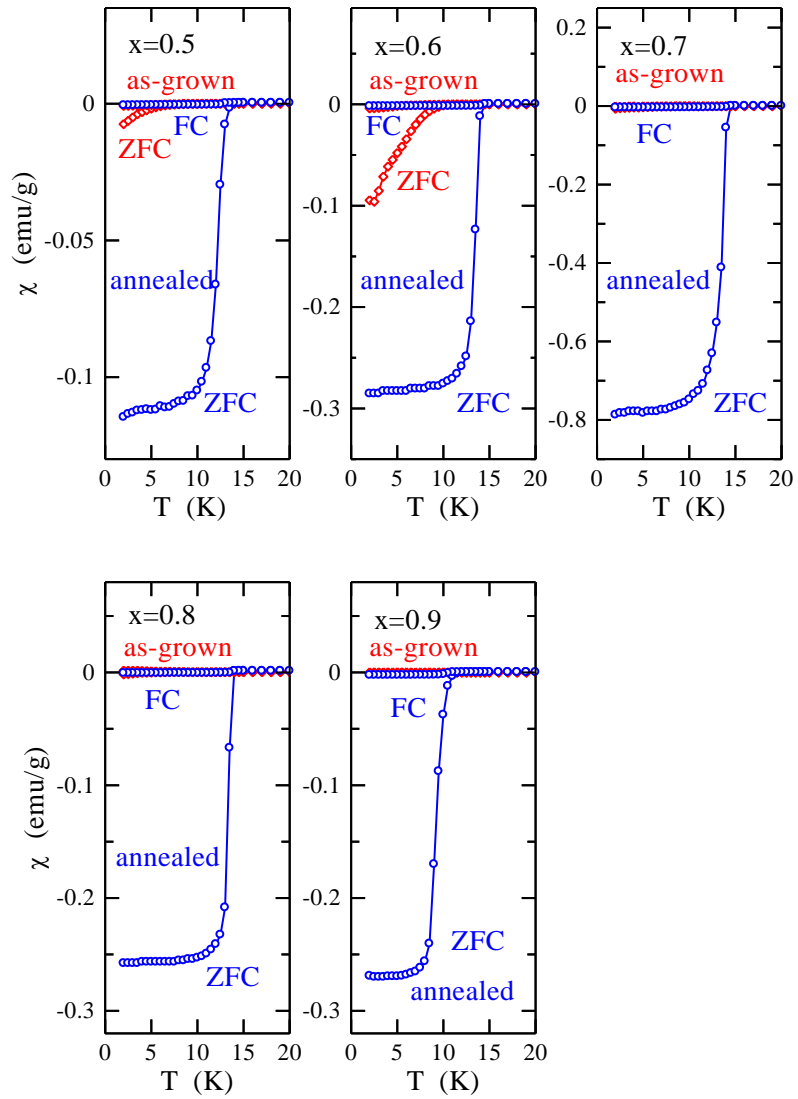


Fig. 3. (Color online) Temperature dependence of the magnetic susceptibility, χ , in a magnetic field of 1 mT parallel to the c-axis on zero-field cooling (ZFC) and field cooling (FC) for as-grown and annealed single-crystals of $\text{FeSe}_{1-x}\text{Te}_x$ with $x = 0.5 - 0.9$.

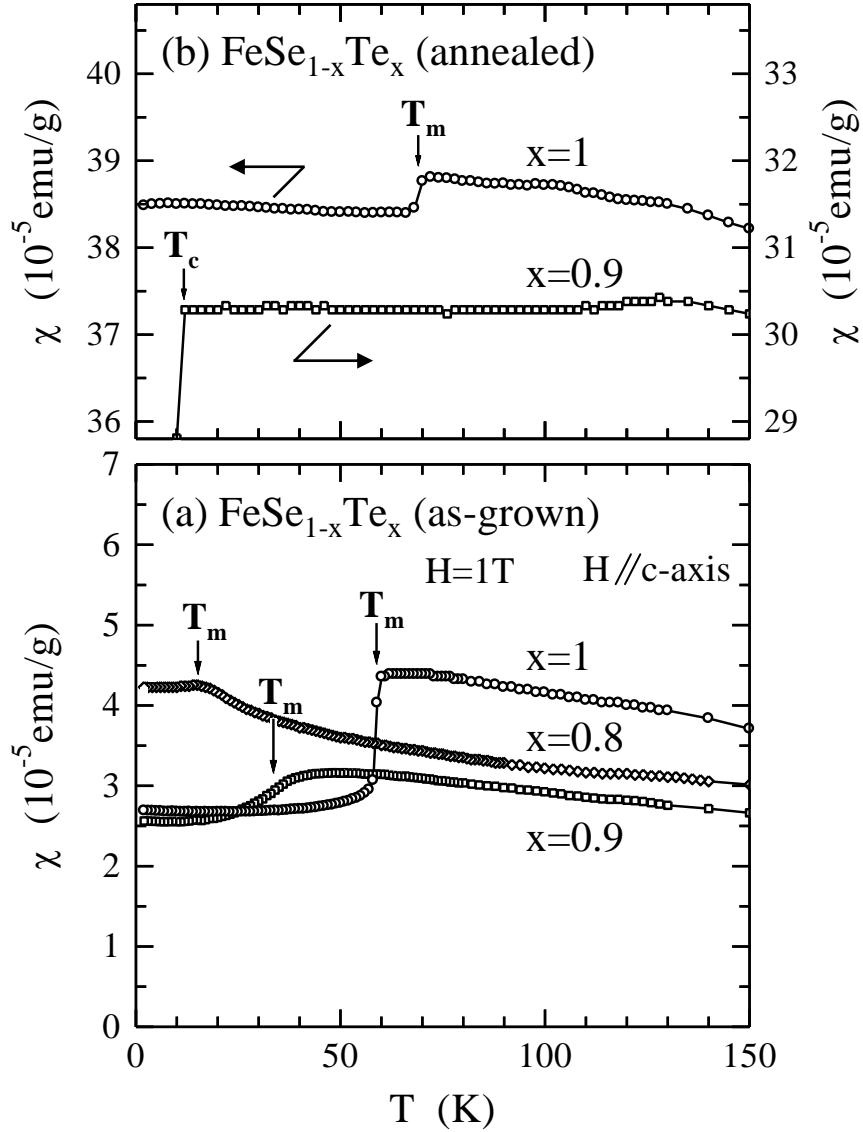


Fig. 4. Temperature dependence of the magnetic susceptibility, χ , in a magnetic field of 1 T parallel to the c -axis for (a) as-grown and (b) annealed single-crystals of FeSe_{1-x}Te_x with $x = 0.8 - 1$. Arrows indicate the magnetic transition temperature, T_m , and the superconducting transition temperature, T_c .

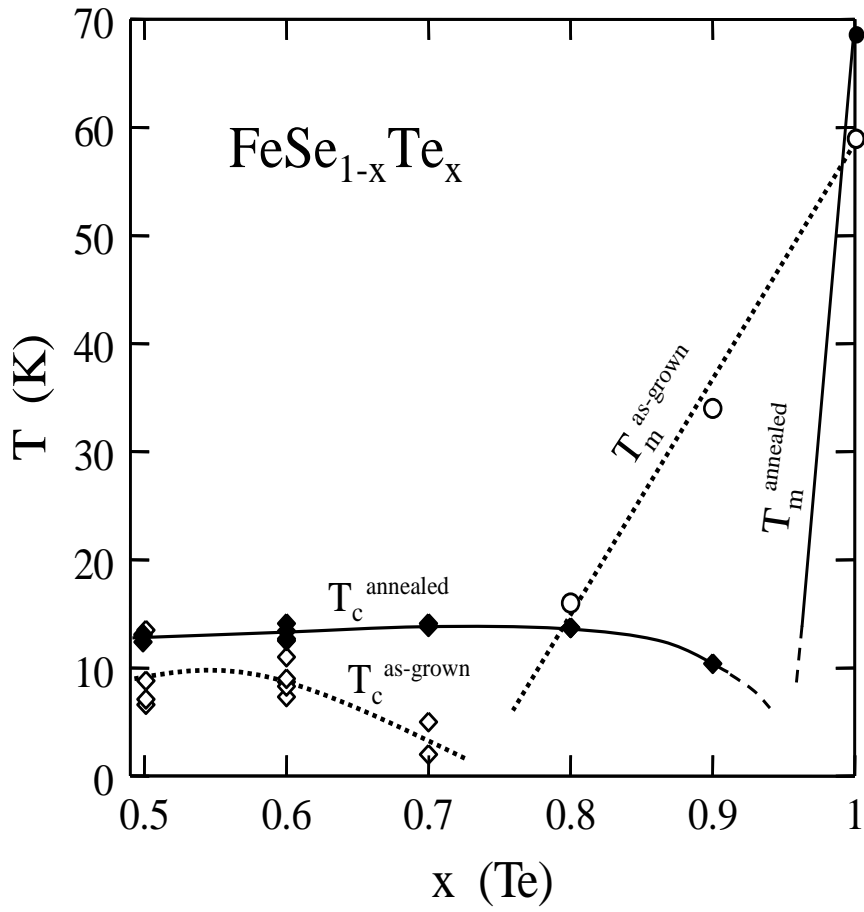


Fig. 5. Dependences on x of the superconducting transition temperature, T_c , and the magnetic transition temperature, T_m , for as-grown and annealed single-crystals of $\text{FeSe}_{1-x}\text{Te}_x$ ($0.5 \leq x \leq 1$).

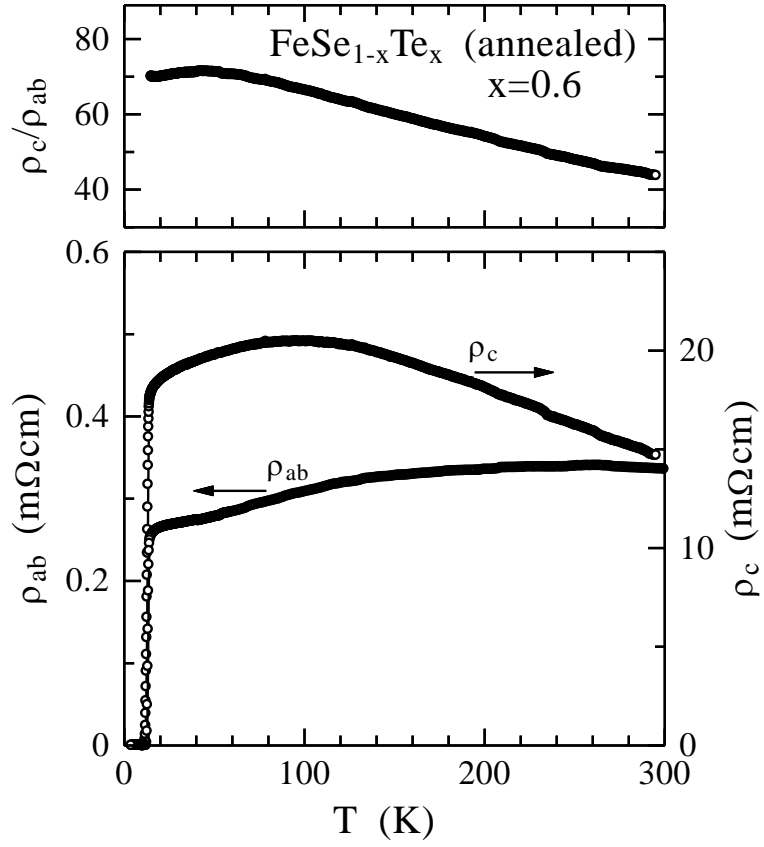


Fig. 6. Temperature dependence of the in-plane electrical resistivity, ρ_{ab} , and the out-of-plane one, ρ_c , (the bottom panel), and the resistivity ratio, ρ_c/ρ_{ab} , (the top panel) for the annealed single-crystal FeSe_{1-x}Te_x with $x = 0.6$.

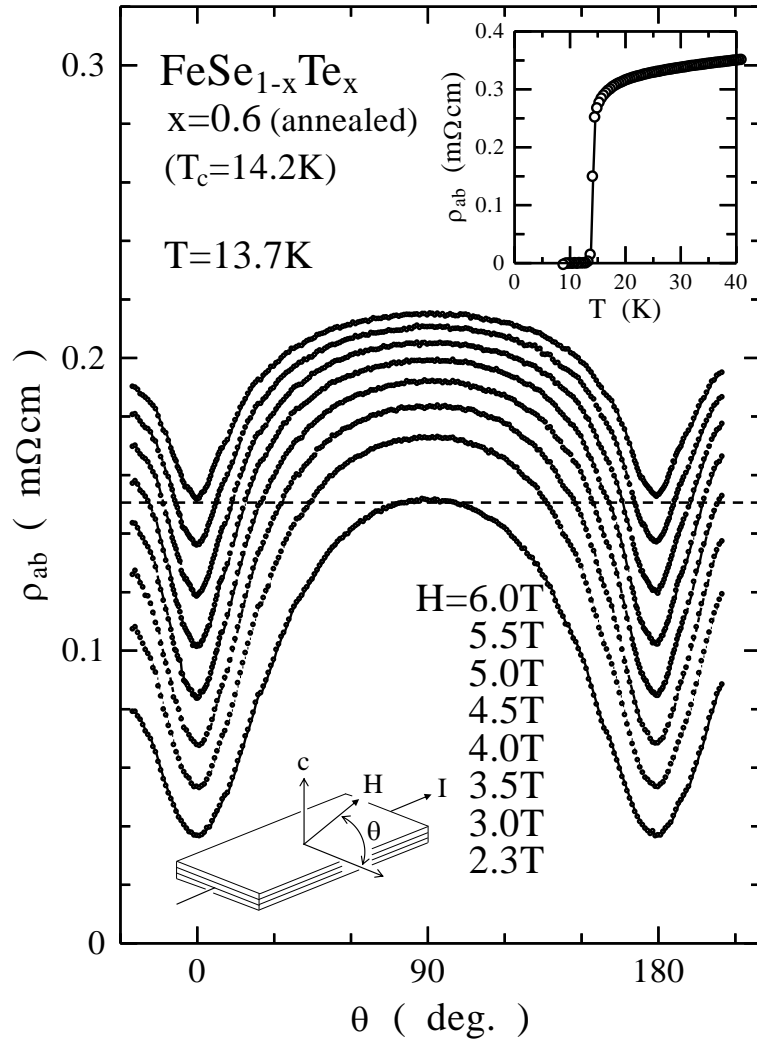


Fig. 7. Dependence of ρ_{ab} on the angle between the ab-plane and the magnetic field direction, θ , under various constant magnetic fields for the annealed single-crystal $\text{FeSe}_{1-x}\text{Te}_x$ with $x = 0.6$. The dashed straight line indicates the half of the normal-state value of ρ_{ab} in zero field. The inset shows the resistive superconducting transition in ρ_{ab} at low temperatures in zero field.

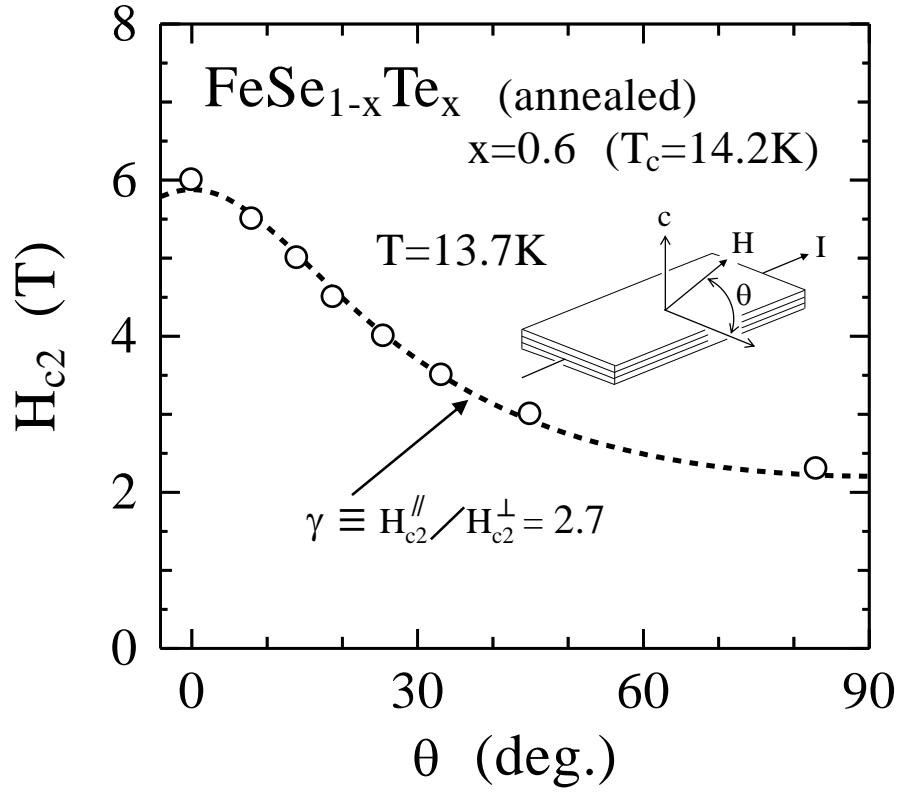


Fig. 8. Angular dependence of H_{c2} , defined at the half of the normal-state value as shown in Fig. 7, for the annealed single-crystal $\text{FeSe}_{1-x}\text{Te}_x$ with $x = 0.6$. The dashed curve indicates the best-fit result obtained using $H_{c2}(\theta) = H_{c2}^{\parallel} (\cos^2\theta + \gamma^2 \sin^2\theta)^{-1/2}$ with $H_{c2}^{\parallel} = 5.9$ T and $\gamma = 2.7$.